



Numerical magnetic field analysis and signal processing for fault diagnostics of electrical machines

Numerical magnetic field analysis

969

S. Pöyhönen

*Department of Automation and Systems Technology,
Control Engineering Laboratory, Helsinki University of Technology,
Finland*

M. Negrea, P. Jover and A. Arkkio

*Department of Electrical Engineering, Laboratory of Electromechanics,
Helsinki University of Technology, Finland*

H. Hyötyniemi

*Department of Automation and Systems Technology,
Control Engineering Laboratory, Helsinki University of Technology,
Finland*

Keywords *Condition monitoring, Electromagnetic fields, Electrical machines, Finite element method, Signal processing, Fault analysis*

Abstract *Numerical magnetic field analysis is used for predicting the performance of an induction motor and a slip-ring generator having different faults implemented in their structure. Virtual measurement data provided by the numerical magnetic field analysis are analysed using modern signal processing techniques to get a reliable indication of the fault. Support vector machine based classification is applied to fault diagnostics. The stator line current, circulating currents between parallel stator branches and forces between the stator and rotor are compared as media of fault detection.*

Introduction

Companies dealing with electrical machinery find condition monitoring and diagnostics more and more important. The supervision of electrical drive systems using non-invasive condition monitoring techniques is becoming a state-of-the-art method for improving the reliability of electrical drives in many branches of the industry.

Typical questions are, how to detect a starting fault, how to distinguish a deteriorating fault from a harmless constructional asymmetry, which are the physical quantities that best indicate a fault and how to measure them, and how should the measured signals be processed to get the most reliable diagnosis.

The basis of any reliable diagnostic method is an understanding of the electric, magnetic and mechanical behavior of the machine in healthy-state and under fault conditions. The aim of computer simulation of magnetic field



distribution and operating characteristics is to foresee the changes of motor performance due to the changes of parameters as a consequence of different faults. Simulation results represent the contribution to the correct evaluation of the measured data in diagnostic procedures, which are the important part of supervision system based on expert systems and artificial intelligence methods (Filipetti *et al.*, 1995).

Concerning the fault indicators, even though thermal and vibration monitoring have been utilized for decades, most of the recent research has been directed toward electrical monitoring of the motor with emphasis on inspecting the stator current of the motor because it has been suggested that stator current monitoring can provide the same indications without requiring access to the motor (MCS, 1992). In particular, a large amount of research has been directed towards using the stator current spectrum to sense specific rotor faults (Benbouzid, 1997; Kliman, 1990). In processing plants, within electrical drives the vibration monitoring is utilized to detect the mechanical faults of rotating electrical machines. The vibration monitoring has been used also to detect the electromechanical faults like broken or cracked rotor bars in squirrel-cage induction motors (Muller and Landy, 1996).

Different kinds of artificial intelligence based methods have become common in fault diagnostics and condition monitoring. For example, fuzzy logic and neural networks (NN) have been used in modeling and decision making in diagnostics schemes. Also, numerical classification methods are widely used in the area of modern fault diagnostics, and in particular, fault diagnostics of electrical machines. For example, in Alguindigue *et al.* (1993) and Li *et al.* (2000), used NN based classifiers in the diagnosis of rolling element bearings.

Support vector machine (SVM) based classification is a relatively new classification method, and it is claimed to have better generalization properties than NN based classifiers. Another interesting feature of SVM based classifier is that its performance does not depend on the number of attributes of classified entities, i.e. dimension of classified vectors. That is why it is noticed to be especially efficient in large classification problems. In fault diagnostics process, this property is very useful, because the number of attributes chosen to be the base of diagnostics is thus not limited.

SVM had been for the first time successfully applied to fault diagnostics of electrical machines in Pöyhönen *et al.* (2002). There we used SVM's to classify faults of a 15 kW induction motor from the stator line current. In the present paper, the method is extended to classify several faults of a 1.6 MVA slip-ring generator and 35 kW cage induction motor. We extend our study concerning the media for fault detection to the analysis of the circulating currents on parallel branches and forces acting on the rotor.

Numerical model for fault simulations*Electromagnetic model of a machine*

The magnetic field in the core of the machine is assumed to be two-dimensional. The three-dimensional end-region fields are modeled approximately using end-winding impedances in the circuit equations of the windings. The magnetic vector potential A satisfies the equation

$$\nabla \times (\nu \nabla \times A) = J \quad (1)$$

where ν is the reluctivity of the material and J is the current density. The current density can be expressed as a function of the vector potential and the electric scalar potential ϕ

$$J = -\sigma \frac{\partial A}{\partial t} - \sigma \nabla \phi \quad (2)$$

where σ is the conductivity of the material. In the two-dimensional model, the vector potential and the current density have only the z -components

$$A = A(x, y, t) e_z \quad (3)$$

$$J = J(x, y, t) e_z$$

The scalar potential ϕ has a constant value on the cross-section of a two-dimensional conductor, and it is a linear function of the z -coordinate. The gradient of the scalar potential can be expressed with the aid of the potential difference u induced between the ends of the conductor. By substituting equation (2) in equation (1) the field equation becomes

$$\nabla \times (\nu \nabla \times A) + \sigma \frac{\partial A}{\partial t} = \frac{\sigma}{\ell} u e_z \quad (4)$$

where ℓ is the length of the conductor. A relation between the total current i and the potential difference u is obtained by integrating the current density (equation (2)) over the cross-section of the conductor

$$u = Ri + R \int_S \sigma \frac{\partial A}{\partial t} dS \quad (5)$$

where R is the dc resistance of the conductor. The circuit equations for the damping cage are constructed by applying Kirchhoff's laws and equation (5) for the potential difference.

Time-dependence. A time-dependent field is solved by discretizing the time at short time intervals Δt and evaluating the field at time instants $t_1, t_2, t_3, \dots (t_{k+1} = t_k + \Delta t)$. In the Crank-Nicholson method, the vector potential at time t_{k+1} is approximated

$$A_{k+1} = \frac{1}{2} \left\{ \frac{\partial A}{\partial t} \Big|_{k+1} + \frac{\partial A}{\partial t} \Big|_k \right\} \Delta t + A_k \quad (6)$$

By adding the field equations written at times t_k and t_{k+1} together and substituting the sum of the derivatives from equation (6), the equation

$$\begin{aligned} \nabla \times (\mathbf{v}_{k+1} \nabla \times A_{k+1}) + \frac{2\sigma}{\Delta t} A_{k+1} = \frac{\sigma}{\ell} u_{k+1} e_z \\ - \left\{ \nabla \times (\mathbf{v}_k \nabla \times A_k) - \frac{2\sigma}{\Delta t} A_k - \frac{\sigma}{\ell} u_k e_z \right\} \quad (7) \end{aligned}$$

is obtained. The time discretization of the potential difference equation (5) gives

$$\frac{1}{2}(u_{k+1} + u_k) = \frac{1}{2}R(i_{k+1} + i_k) + R \int_S \frac{A_{k+1} - A_k}{\Delta t} dS \quad (8)$$

Equations (7) and (8) form the basic system of equations in the time-stepping formulation. Starting from the initial values and successively evaluating the potentials and currents of the next time-steps, the time variation of the quantities is worked out.

Numerical solution. The construction of the circuit equations and the details of the numerical solution of the coupled field and circuit equations have been presented by Arkkio (1988). The finite element discretization leads to a large non-linear system of equations in which the unknown variables are the nodal values of the vector potential and the currents or potential differences of the windings. The equations are solved by the Newton-Raphson method.

Finite element mesh. The magnetic field of a healthy electrical machine is periodic, typically from one pole pair to the next one. A fault in the machine disturbs this symmetry, and the whole machine cross section has to be modeled. For fault detection purposes, we are more interested in qualitative than exact quantitative results, and the finite element meshes used can be relatively sparse, as long as the geometric symmetry is the same as for the faulty machine. In this study, triangular first-order finite elements are used, and the finite element meshes typically contain 6,000-8,000 elements.

Motion of the rotor. In a general time-stepping analysis, the equations for rotor and stator fields are written in their own reference frames. The solutions of the two field equations are matched with each other in the air gap. The rotor is rotated at each time-step by an angle corresponding to the mechanical angular frequency. The rotation is accomplished by changing the finite element mesh in the air gap.

Operating characteristics. The magnetic field, the currents and the potential differences of the windings are obtained in the solution of the coupled field and

circuit equations as discussed earlier. Most of the other machine characteristics can be derived from these quantities.

Modeling the faults

The faults studied in the numerical simulations are:

- shorted turn in stator winding (ST)
- shorted coil in stator winding (SC)
- shorted turn in rotor winding (slip-ring generator) (RT)
- shorted coil in rotor winding (slip-ring generator) (RC)
- broken rotor bar (cage induction motor) (BB)
- broken end ring (cage induction motor) (BR)
- static or dynamic rotor eccentricity (SE, DE)
- asymmetry in line voltage (slip-ring generator) (VA)

To model a shorted turn, the sides of this turn in the finite element mesh are substituted by conductors in perfect short-circuit. There is no galvanic contact between the reduced phase winding and the new, shorted conductors. A shorted coil is treated in a similar manner.

Static eccentricity is obtained by shifting the rotor by 10 percent of the radial air-gap length, and rotating the rotor around its center point in this new position. Dynamic eccentricity is obtained by shifting the rotor by 10 percent of the air-gap length, but rotating it around the point that is the center point of the stator bore. A 10 percent eccentricity is not yet a real fault, but an eccentricity possibly growing should be detected at an early stage.

The circuit equations of the cage winding are composed of the potentials of the bars inside the rotor core, bar ends outside the core and end ring segments connecting the bars. When modeling a broken bar, the resistance of the bar end outside the core is increased to a value 100 times the dc resistance of the whole bar. When modeling a broken end ring, the resistance of an end-ring segment between two bars is increased to a value 1,000 times the original resistance of the segment.

An asymmetry in the line voltage is not a fault (NF) in the machine, but it may cause problems if the fault diagnostics algorithms identify the voltage asymmetry as a machine fault. The asymmetric voltage is obtained by adding 5 percent of negative phase-sequence voltage to an originally 100 percent positive phase-sequence supply voltage.

Fault indicators

The parameters studied as fault indicators are line currents, circulating currents between parallel stator branches, and force between the stator and rotor.

To compute the stator currents, the parallel branches are treated as separate phases. If there are n parallel branches, the machine is treated as a $3n$ -phase machine supplied from a $n \times 3$ -phase voltage source. In the case of a star connection, all the $3n$ phases have a common star-point, and a line current is obtained as the sum of n branch currents. A circulating current is half of the difference of two branch currents.

The electromagnetic force acting between the stator and rotor is computed from the air-gap field using the method developed by Coulomb (1983).

SVM for multi-class classification

SVM based classification is a relatively new machine learning method based on the statistical learning theory presented by Vapnik (1998). In SVM, an optimal hyperplane is determined to maximize the generalization ability of the classifier by mapping the original input space into a high dimensional dot product space called feature space. The mapping is based on the so-called kernel function. The optimal hyperplane is found in the feature space with a learning algorithm from optimization theory, which implements a learning bias derived from statistical learning theory (Cristianini and Shawe-Taylor, 2000).

A SVM based classifier is a binary classifier. In fault diagnostics of an electrical machine, there exist several fault classes in addition to healthy operation. We need a method to deal with a multi-class classification problem. In this study, we use a mixture matrix approach that is suggested by Mayoraz and Alpaydin (1999).

SVM is used to build pair-wise classifiers for all considered classes. For an n -class classification problem $n(n - 1)/2$ pair-wise classifiers cover all pairs of classes. Each classifier is trained on a subset of the training set containing only training examples of the two involved classes. Final solution to the n -class problem is reconstructed from solutions of all two-class problems.

Often, simple majority voting between pair-wise classifiers is applied to reconstruct the n -class solution, but with this approach problems occur, if two separate classes get equal amount of votes. Majority voting approach does not take into account possible redundancy in pair-wise classifiers' outputs. With a mixture matrix approach, the n -class solution is found by linear combination of pair-wise classifiers' solutions. The mixture matrix is designed in the training phase of classifiers to minimize the mean square error between the correct class decision and the linear combination of pair-wise classifiers' outputs.

Preprocessing data

Power spectra estimates of the stator line currents have often been used as a medium of fault detection of electrical machines (Benbouzid, 1997). Main disadvantage of classical spectral estimation techniques, like FFT, is the impact of side lobe leakage due to windowing of finite data sets. Window weighting decreases the effect of side lobes. Further, in order to improve

the statistical stability of the spectral estimate, averaging by segmenting the data can be applied. The more segments are used, the more stable the estimate is. However, the signal length limits the number of segments used, but with overlapping segments the number of segments can be increased. In this study, Welch's method is used to calculate the power spectra estimates of signals in motors. The method applies both the window weighting and the averaging over overlapping segments to estimate the power spectrum. In this study, we use Hanning window sized 500 samples, and number of overlapping samples is 250.

Before estimating the power spectra, adaptive predictive filtering is applied to mitigate the impact of noise (Väliviita *et al.*, 1999). Noise filtering is applied only in the case where stator line current is used as a medium of fault detection.

Simulation results

Numerical analysis

Table I gives the main parameters of the cage induction motor and slip-ring generator. In the present study, the cage induction motor was fed from a frequency converter. The stator and rotor windings of the slip-ring generator were connected to sinusoidal voltage sources. The stator is delta connected and the rotor is star connected. Figure 1 shows the cross-sectional geometry of the slip-ring machine. Figures 2 and 3 show two examples of simulated circulating currents flowing in the parallel stator branches. The current in Figure 2 is caused by 10 percent dynamic eccentricity in the slip-ring generator operating at a capacitive power factor of 0.8 at half load. Figure 3 shows the circulating current in the cage induction motor with one broken rotor bar and loaded by the rated torque. The rated currents of the machines are 1,600 and 62 A, respectively.

Figures 4 and 5 show the x -components of the forces acting between the stator and rotor for the slip-ring generator with the 10 percent dynamic eccentricity and for the cage induction motor with a broken rotor bar, respectively.

	Induction motor	Slip-ring generator
Number of poles	4	4
Parallel branches	2	4
Stator connection	Star	Delta
Rotor connection	–	Star
Rated power (kW)	35	1,600
Rated frequency (Hz)	100	50
Rated voltage (V)	400	690
Rated current (A)	64	1,500

Table I.
Main parameters of
the studied electrical
machines

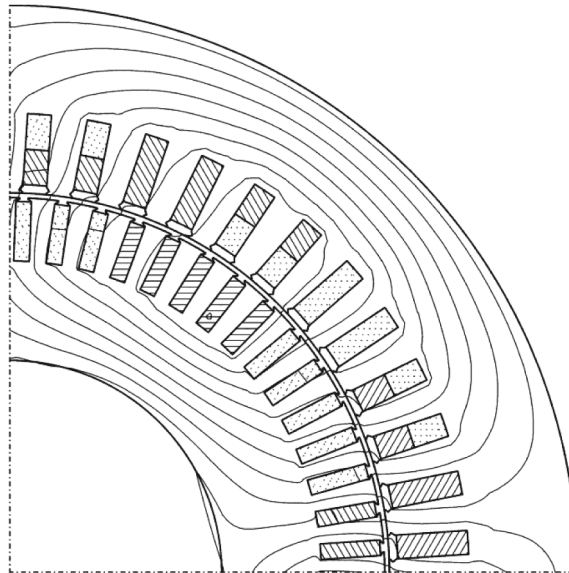


Figure 1.
Cross-sectional geometry
of the slip-ring generator

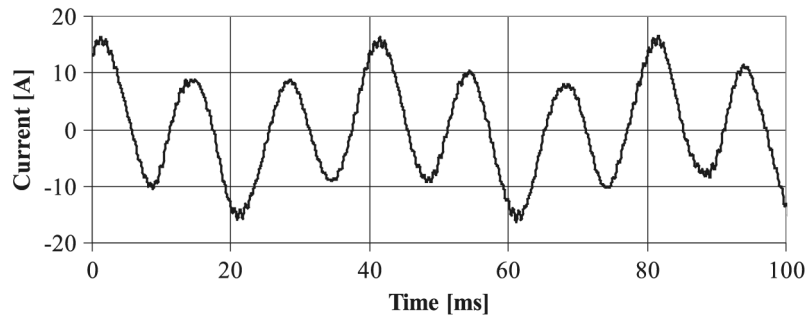


Figure 2.
Circulating currents
flowing in parallel
branches of the stator
windings for the slip-ring
generator with 10 percent
dynamic eccentricity

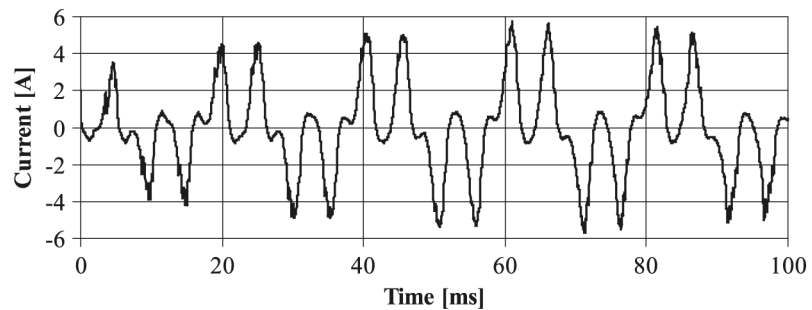


Figure 3.
Circulating currents
flowing in parallel
branches of the stator
windings for the cage
induction motor with one
broken rotor bar

Support vector machine based classification

Generating the sample set. Measurement error is included to the virtual measurement data by adding noise to the signals. Mean value of noise is zero and variance is 3 percent of the amplitude of the current.

The power spectrum estimates are calculated 80 times from different parts of signals in each fault case to generate a sample set. The support vector classifiers are trained and tested separately in different load situations. Half of the samples are chosen for training the classifier, and half of the samples are left for testing the classifier's generalization ability. An average healthy spectrum from the training set is chosen to be a reference, and all the other spectra are scaled with it. The difference values from the reference create the sample set.

Classification results. We have six fault classes and the healthy class, so $n = 7$, and we need to design 21 two-class classifiers that are combined to generate the final classification decision for a spectrum sample. Choosing the kernel function used in building, the SVMs have a considerable influence on the classification results. There does not exist general rules for choosing the kernel function, but the best kernel function depends on the application where SVMs are used. When the cage induction motor was studied, all classifiers were designed with a radial basis kernel function width equal to 11 except when studying forces as indicators of faults. When the slip-ring machine was studied,

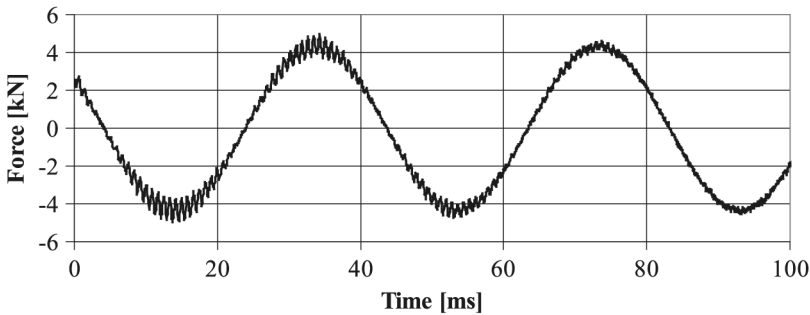


Figure 4.
Force acting between the stator and rotor for the slip-ring generator with 10 percent dynamic eccentricity

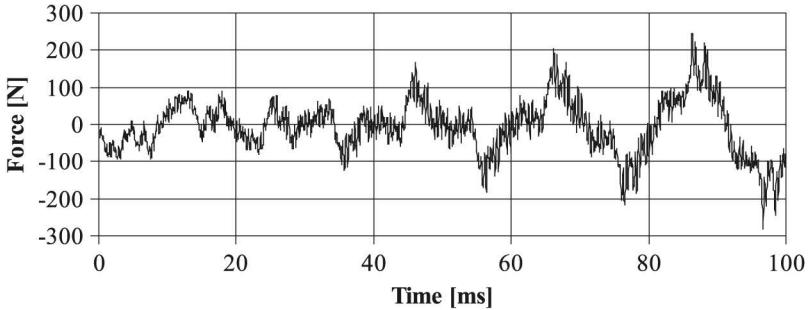


Figure 5.
Force acting between the stator and rotor for the cage induction motor with one broken rotor bar

The circulating currents and the force on the rotor are natural fault indicators as they are zero for all healthy symmetric machines, but non-zero for faults that cause asymmetry in the magnetic field distribution of a machine.

The stator line current is also a good indicator of faults in noiseless situation, but in real world applications noise is always present. Shorted turn and shorted coil in stator are always detected regardless of noise. However, healthy operation is often misclassified. Thus, stator line current cannot be used as medium of fault detection without improvements on the classification method or in noise filtering. Dropping such fault classes out of the classification structure that cannot be separated from the healthy operation, we could construct a classifier that is able to correctly detect healthy operation and shorted coil and shorted turn faults from the stator line current. Also other ways of estimating the power spectrum of the current may give some enhancement.

Percent	NF	NF/VA	RC	RT	ST	SC	SE	DE	Total
C	40	0	25	73	100	100	15	15	46
O	28	0	100	63	100	100	25	35	56
S	35	0	35	53	100	100	33	48	50
U	38	0	100	100	100	100	15	48	63
Total	35	0	65	72	100	100	22	37	54

Table V.
Correct fault
classification
percentages of
slip-ring generator,
stator line current as
a medium of fault
detection

Percent	NF	NF/VA	RC	RT	ST	SC	SE	DE	Total
C	100	100	50	100	100	100	100	100	94
O	100	100	100	100	100	100	100	100	100
S	100	100	100	100	100	100	100	100	100
U	100	100	100	100	100	100	100	100	100
Total	100	100	88	100	100	100	100	100	99

Table VI.
Correct fault
classification
percentages
slip-ring generator,
circulating currents
between parallel
branches as media
of fault detection

Percent	NF	NF/VA	RC	RT	ST	SC	SE	DE	Total
C	100	100	100	45	100	100	100	100	93
O	100	100	100	100	100	100	100	100	100
S	100	100	100	88	100	100	100	100	98
U	100	100	100	100	100	100	100	100	100
Total	100	100	100	83	100	100	100	100	98

Table VII.
Correct fault
classification
percentages of a
slip-ring generator,
force on the rotor as
a medium of fault
detection

Notes: C = base speed, power factor 0.8 capacitive; O = 1.12 × base speed, resistive load; S = base speed, resistive load; U = 0.88 × base speed, resistive load.

Experimental results

The 35 kW cage induction motor was fed from an inverter having a switching frequency of 3 kHz. A DC generator was used for loading the motor. The currents, voltages, power and supply frequency were measured using a wide band power analyzer. The measurements were carried out for three different load conditions. Figure 6 presents a schematic view of the measuring set-up.

The current and voltage waveforms were recorded with a transient recorder. Hall sensors (LEM) were used as current transducers, and the voltages were measured through an isolation amplifier. The sampling frequency was 40 kHz and a typical number of samples was 20,000. The recording system was calibrated using the measurements from the power analyzer.

Healthy operation, broken rotor bar operation and operation under inter-turn short circuit were analyzed. Power spectra estimate samples were calculated from the current, and a SVM classification structure was constructed only for these three classes. If measurement data were used in both training and testing the classifier, all test samples were correctly classified in all load situations (Table VIII).

Conclusions

Numerical magnetic field analysis was used to provide virtual measurement data from healthy and faulty operation of the machines and support vector

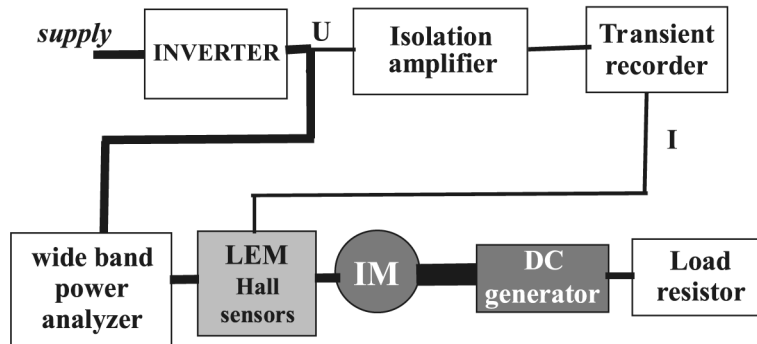


Figure 6.
Schematic of the measuring set-up

Table VIII.
Correct fault classification percentages from the measurements of a cage induction motor, stator current as a medium of fault detection

	NF	BB	ST	Total
Full load	100	100	100	100
Half load	100	100	100	100
No load	100	100	100	100

classification was applied to fault diagnostics of a cage induction motor and a slip-ring generator. Stator line current, circulating currents between parallel branches and forces acting on the machine's rotors were compared as media of fault detection. Circulating currents between parallel branches and forces on rotor were found to be superior indicators of faults compared to the stator current. However, in experimental studies, healthy operation, broken bar operation and operation under inter-turn short circuit were correctly classified based on the stator current, if measurement data were used in both training and testing the classifier.

References

- Alguindigue, I.E., Loskiewicz-Buczak, A. and Uhrig, R. (1993), "Monitoring and diagnosis of rolling element bearings using artificial neural networks", *IEEE Transactions on Industrial Electronics*, Vol. 40 No. 2, pp. 209-17.
- Arkkio, A. (1988), "Analysis of induction motors based on the numerical solution of the magnetic field and circuit equations", Helsinki, Acta Polytechnica Scandinavica, Electrical Engineering Series No. 59, ISBN 951-666-250-1, p. 97.
- Benbouzid, M.E.H. (1997), "Induction motor diagnostics via stator current monitoring," *Proc. 1997 Int. Conf. Maintenance and Reliability*, Knoxville, TN, Vol. 1, pp. 1-10.
- Coulomb, J.L. (1983), "A methodology for the determination of global electromechanical quantities from the finite element analysis and its application to the evaluation of magnetic forces, torques and stiffness", *IEEE Transactions on Magnetics*, Vol. MAG-19 No. 6, pp. 2514-9.
- Cristianini, N. and Shawe-Taylor, J. (2000), *Support Vector Machines and Other Kernel-Based Learning Methods*, Cambridge University Press, Cambridge.
- Filipetti, F., Franceschini, G. and Tassoni, C. (1995), "Neural networks aided on-line diagnostics of induction motor rotor faults", *IEEE Transactions on Industry Applications*, Vol. 31 No. 4.
- Kliman, G.B. (1990), "Induction motor fault detection via passive current monitoring," *Proc. 1990 Int. Conf. Electrical Machines*, Cambridge, MA, Vol. 1, pp. 13-17.
- Li, B., Chow, M.-Y., Tipsuwan, Y. and Hung, J.C. (2000), "Neural-network-based motor rolling bearing fault diagnosis", *IEEE Transactions on Industrial Electronics*, Vol. 47 No. 5, pp. 1060-9.
- Mayoraz, E. and Alpaydin, E. (1999), "Support vector machines for multi-class classification", *IWANN 1999*, Vol. 2, pp. 833-42.
- MCS (1992), "Methods of motor current signature analysis", *Mach. Power Syst.*, Vol. 20, pp. 463-74.
- Muller, H. and Landy, C.F. (1996), "Vibration monitoring for broken rotor bars in squirrel cage induction motors with interbar currents", *SPEEDAM 96*, 5-7 June, Capri, Italy, Vol. A2.
- Pöyhönen, S., Negrea, M., Arkkio, A., Hyötyniemi, H. and Koivo, H. (2002), "Support vector classification for fault diagnostics of an electrical machine," *Proceedings ICSP'02*, 26-30 August, Beijing, China.
- Väliiviita, S., Ovaska, S.J. and Vainio, O. (1999), "Polynomial predictive filtering in control instrumentation: a review", *IEEE Transactions on Industrial Electronics*, Vol. 46 No. 5, pp. 876-88.
- Vapnik, V.N. (1998), *Statistical Learning Theory*, Wiley, New York.